

Nature of Magnetism in III-V based Diluted Magnetic Semiconductors

S. Katsumoto^{1,2}, T. Hayashi¹, Y. Hashimoto¹, Y. Iye^{1,2}, Y. Ishiwata¹, M. Watanabe³, R. Eguchi¹, T. Takeuchi⁴, Y. Harada³, S. Shin^{1,3} and K. Hirakawa^{2,5}

¹*Institute for Solid State Physics, University of Tokyo, 5-1-5 Kashiwanoha, Kashiwa, Chiba 277-8581, Japan*

²*CREST, Japan Science and Technology Corporation, Mejiro, Tokyo 171-0031, Japan*

³*RIKEN/Spring-8, Kouto, Mikazuki-cho, Sayo-gun, Hyogo 679-5143, Japan*

⁴*Department of Applied Physics, Science University of Tokyo, Kagurazaka, Shinjuku-ku, Tokyo 162-8601, Japan*

⁵*Institute of Industrial Science, University of Tokyo, 4-6-1 Komaba, Meguro-ku, Tokyo 153-8505, Japan*

A systematic study on magnetism and transport in III-V based diluted magnetic semiconductors (Ga,Mn)As and (In,Mn)As is presented. Low-temperature annealing effect is utilized to control material parameters. X-ray absorption spectroscopy revealed that Mn-ions that contribute to the ferromagnetism are in d^5 states, hence the holes should mainly be in As $4p$ states. On the other hand, infrared optical conductivity measurements indicate those holes are almost localized. These results naturally provide a picture for the ferromagnetism in these materials. The low-temperature annealing is also applied to detailed study of the metal-insulator transition.

KEYWORD: diluted magnetic semiconductor, infrared conductivity, X-ray absorption spectroscopy

1. Introduction

III-V based diluted magnetic semiconductors (DMSs) are attracting much attention mainly because of their ferromagnetism^{1,2}, which has close relation to electric transport and is controllable by external parameters such as light illumination³ or electric field⁴. While extensive studies on control of the ferromagnetism or other extrinsic effects, physical mechanism of the ferromagnetism is still under debate⁵ and experimental results so far accumulated are not converged satisfactorily.

A main problem for systematic study of the ferromagnetism in these materials is the sensitivity of material parameters to the growth conditions⁶. In order to incorporate magnetic ions such as Mn into III-V materials beyond solubility limits, low-temperature molecular-beam epitaxy (LT-MBE) is usually adopted⁷. In order for the growth far from equilibrium, substrate temperature during the growth is kept much lower than usual growth temperature. As a result, for example, a slight difference in the growth temperature may cause a huge difference in electric transport.

We found that annealing of such III-V DMS films after growth at comparatively low temperatures greatly improves the crystallinity and provides a stable method to synthesize the materials, that is, the quality of resultant films are not only insensitive to the growth conditions but also at highest grade so far reported⁸. This method can also be used to control material parameters in a single wafer by adjusting, e.g. the annealing time⁹.

In this article, we report a study on the properties of (In,Mn)As and (Ga,Mn)As, in which the LT-annealing is fully utilized. That is, the clarification of the origin of the LT-annealing effect should lead to the clarification of the mechanism of the ferromagnetism. The LT-annealing is also applied to metal-insulator transition (MIT), which is another important issue in this material.

2. Experiment

2.1 Sample preparation

The initial (Ga,Mn)As and (In,Mn)As films were grown on 500nm-thick GaAs buffer layers, which were grown on

(001) semi-insulating GaAs substrates at 580C. The growth temperatures for (Ga,Mn)As and (In,Mn)As were 220C and 300C respectively. The V/III (As₄/Ga) ratio was about 3. The thickness of the films was 200nm.

For (Ga,Mn)As, Mn content x was determined from the shift of X-ray diffraction peak with the index (004) assuming that lattice relaxation does not occur. For (In,Mn)As, x was estimated from calibration of the molecular beam of In and Mn.

Low-temperature (LT) annealing were carried out in the atmosphere of N₂ gas. Besides the study of metal-insulator transition, the annealing time was fixed at 15minutes. No change in full-width-at-half-maximum (FWHM) was observed in the X-ray diffraction peak after the annealing in the case of (Ga,Mn)As and the FWHM decreased for (In,Mn)As indicating that the crystallinity was improved.

2.2 Measurement

For the conventional transport measurement in the study of annealing effect, simple van der Pauw method was adopted. The ferromagnetic transition temperature (T_c) was determined by magnetization measurement with a commercial superconducting quantum interference device magnetometer.

The X-ray absorption spectroscopy (XAS) was performed by using a soft-X-ray spectrometer installed at the undulator beamline BL-2C in Photon Factory of KEK. Synchrotron radiation was monochromatized using a varied line spacing plane grating, whose energy resolution was less than 0.1 eV at 650eV. The spectra were taken at room temperatures and at 40K.

For infrared conductivity measurement, the samples were cooled in a He gas flow cryostat. The conductivities were measured in a transmission-geometry by using a Fourier transform spectrometer. The optical absorption coefficient $\alpha(\omega)$ of the epitaxial film (Ga,Mn)As is expressed by the transmission spectrum of the insulating GaAs substrate t_{GaAs} and that of the film t_{GaMnAs} as

$$\alpha(\omega) = d^{-1} \log \left(\frac{t_{\text{GaAs}}}{t_{\text{GaMnAs}}} \right)$$

where d is the thickness of the film.

The transmission spectra are also connected to the optical conductivity $\sigma(\omega)$ through

$$\frac{t_{\text{GaAs}}}{t_{\text{GaMnAs}}} = \left| 1 + \frac{\sigma(\omega)d}{Y_0 + Y_s} \right|^2,$$

where Y_0 and Y_s are the admittances of the vacuum and GaAs, respectively.

In order to study MIT, a (Ga,Mn)As film with $x=0.05$ was formed into a Hall-bar shape by photolithography. The as-grown wafer was insulating. The annealing time was adjusted to bring the sample close to the MIT critical point. The specimen was cooled down to 0.05K in a mixing chamber of a dilution refrigerator. Magnetic field up to 15T was applied to make the sample go through the critical point.

3. Results and Discussion

3.1 Effect of LT-annealing

Figure 1 shows the temperature dependence of the resistivity in (Ga,Mn)As with $x=0.05$. The as-grown sample shows typical insulating manner besides a hump structure around 40K. This structure is known to appear at about T_C . With increasing the annealing temperature, the resistivity surprisingly decreased and the hump structure shifted to higher temperatures.

Figure 2 summarizes the effect of LT-annealing. The hole concentration p estimated from the room temperature Hall coefficient and T_C have maxima at about 260C, T_C at the maximum is almost the highest in those reported so far. Even with lower T_a , a similar value of T_C can be achieved with elongation of the annealing time. Quality of the resultant films is insensitive to the MBE growth conditions, or to the annealing ones. Hence this ‘‘LT-MBE plus LT-annealing’’ method is stable against the growth conditions.

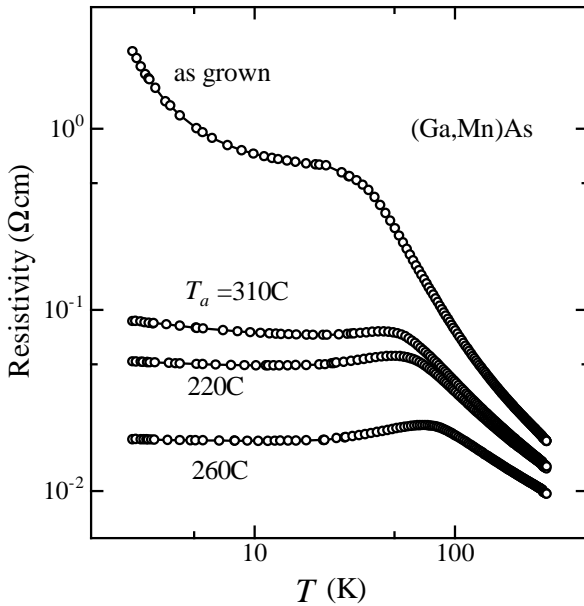


Fig.1. Temperature dependence of resistivity for as-grown and LT-annealed (Ga,Mn)As with $x=0.05$.

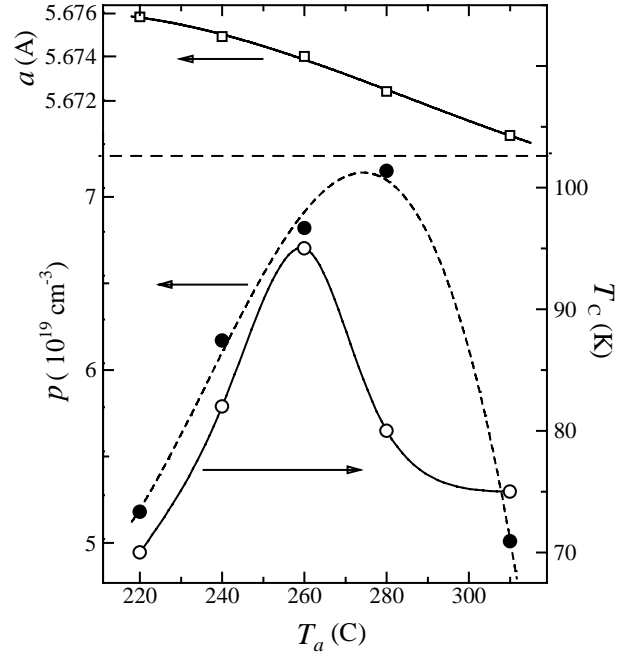


Fig.2 Ferromagnetic transition temperature (T_C), hole concentration (p) and lattice constant (a) versus annealing temperature (T_a) for (Ga,Mn)As with Mn content 0.05

The LT-annealing enhances T_C without varying the Mn concentration. Hence the search for the origin of the LT-annealing effect is expected to be directly related to the mechanism of ferromagnetic order.

3.2 X-ray absorption spectroscopy

XAS is a powerful technique to investigate site-projected density of states and is free from artifacts due to surfaces. We used the wavelength of Mn $2p \rightarrow 3d$ transition thus the obtained spectrum directly reflects the local density at Mn ions.

The upper curve in Fig.3(a) is an XAS spectrum of a LT-annealed sample. The structures around 640eV and 651eV correspond to L_3 and L_2 levels respectively. This spectrum is very similar to a Mn $2p$ XAS calculation based on atomic

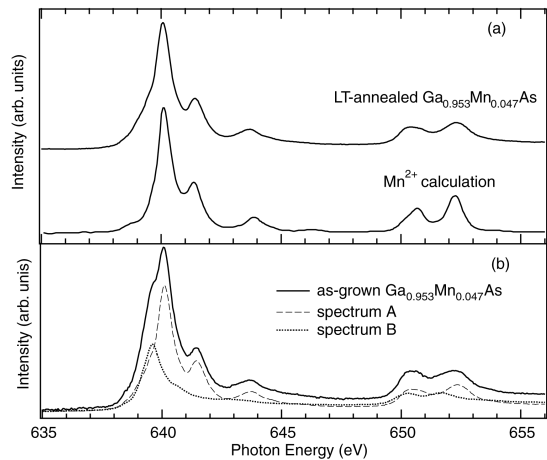


Fig.3. (a) XAS spectrum for LT-annealed (Ga,Mn)As and calculated one for d^5 (b) Decomposition of a spectrum

multiplet theory for $\text{Mn}^{2+}(d^5)$ in tetrahedral (T_d) coordination for the case with crystal-field strength ($10Dq$) 0.5eV, manifesting Mn is in T_d symmetry. We call the spectrum of this LT-annealed sample for $x=0.047$ “spectrum A”. An advantage in XAS is as can be seen above, qualitative comparison can be led to unambiguous information of electronic states.

The main peak (L_3) in the as-grown samples has a doublet structure, which consists of peaks at 639.5eV and 640eV. Assuming that this doublet contains spectrum-A, we can decompose the doublet into two d^5 -like spectra, spectrum-A and spectrum-B.

Figure 4 shows relative intensity of these absorption spectra as a function of Mn content. T_C is also shown for comparison. Apparent correlation between the intensity of spectrum-A and T_C indicates that spectrum-A is produced by Mn ions that participate in the ferromagnetism. Spectrum-B probably comes from Mn ions passivated by neighboring excess As atoms¹⁰.

The fact that spectrum-A contains no d^4 -like spectrum, the above results suggest that the holes emitted from Mn almost exist in the As 4*p* band. This is rather against a simple hypothesis that *d*-holes mediate the ferromagnetism through the double-exchange mechanism.

3.3 Infrared optical conductivity

Low-energy optical conductivity would give information complement to the above XAS. Figure 5 shows infrared optical conductivity of (Ga,Mn)As with $x=0.052$ for as-grown and LT-annealed samples.

The most characteristic feature in this figure is the broad peak structure around 200meV. Such peak structure indicates that the emitted holes are almost localized and the conduction is hopping-like rather than free-carrier picture adopted in RKKY-like model for the ferromagnetism. The

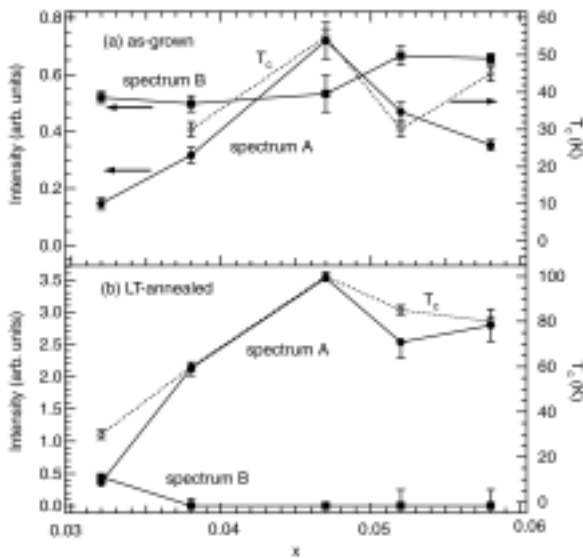


Fig.4. Relative intensity of XAS spectra named “spectrum A” and “spectrum B” (see Fig.3(b)) for (a) as-grown samples and (b) LT-annealed samples as a function of Mn content.

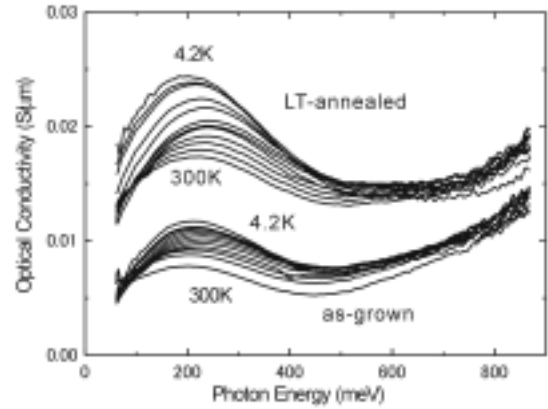


Fig.5 Infrared optical conductivity of as-grown ($T_C=40\text{K}$) and LT-annealed ($T_C=95\text{K}$) (Ga,Mn)As with $x=0.05$. Temperatures are 4.2, 10, 20, 30, 40, 60, 80, 100, 150, 200, 250 and 300K.

conductivity at this peak was greatly enhanced with the LT-annealing and at the same time T_C was enhanced from 40K to 90K¹¹.

The strong correlation between the peak conductivity and T_C indicates that the peak originates from the carriers that mediate the ferromagnetic interaction, though the true origin of the peak structure is still under debate.

Integrating the above information, we conclude that the ferromagnetism is mediated by holes mainly in As 4*p* band, which are almost localized. We can further deduce that the mechanism of the interaction is more double-exchange like rather than RKKY type. Hence we can outline a scenario for the ferromagnetism as follows. Mn acceptors emit holes into As 4*p* band, though they are almost localized and strongly coupled to localized moment at Mn ions through *p-d* mixing. The order of local moments enables the hopping between the nearly localized sites gaining kinetic energy of holes. This mechanism is essentially based on the double-exchange interaction.

This deduction has further support shown in Fig.6, which displays temperature dependent component of the absorption coefficient ($\alpha(T)-\alpha(T_C)$) below 100K for a sample with $x=0.05$ and T_C of 110K. Below T_C , spectrum-weight transfer to low-energy region, which is characteristic in systems of double-exchange-ferromagnetism. We may say that the above scenario is rather close to “double-resonance” mechanism⁵.

We also measured optical conductivity in (In,Mn)As with various Mn content. The spectra are much more like ordinal Drude-type, manifesting the holes are more delocalized.

LT-annealing of these materials again caused large enhancement in hole concentration and conductivity. However T_C was not enhanced so much as expected. This result suggests that holes that have larger mobility and Drude-like transport properties have smaller *p-d* exchange constant and do not contribute to the ferromagnetism. Hence the

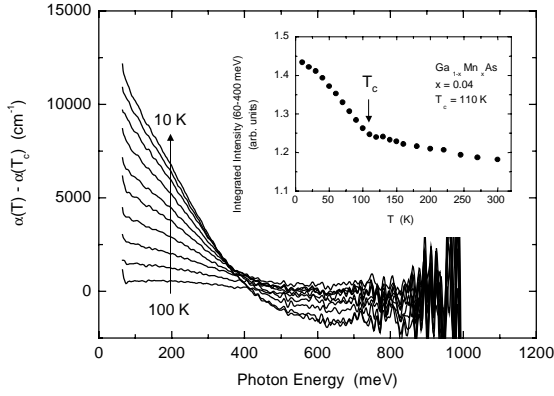


Fig.6 Spectral-weight transfer below T_C (110K) in (Ga,Mn)As with $x=0.04$. The temperature step is 10K.

situation is rather complicated that the weak localization of holes enhances the p - d mixing while complete localization disturbs the ferromagnetism.

3.4 Metal-insulator transition

The above mechanism of ferromagnetism has close relation with the nature of the MITs. III-V-based DMSs are known to have insulator-metal-insulator re-entrant transition¹²⁾. The first insulator-to-metal transition is associated with appearance of ferromagnetism. Hence the first MIT has complicated mechanism as seen in the previous subsections. On the other hand, the second MIT is comparatively simple disorder-driven type.

This would result in difference in the scaling properties. The scaling properties for the relevant parameter z and the temperature T can be summarized in the formula

$$\sigma(z, T) = T^w f(|z/z_c - 1|/T^y)$$

where σ is the conductivity, f is a scaling function, w and y are parameters giving the critical exponent $\nu=w/y$.

Figure 7 shows an example of fitting by using the above

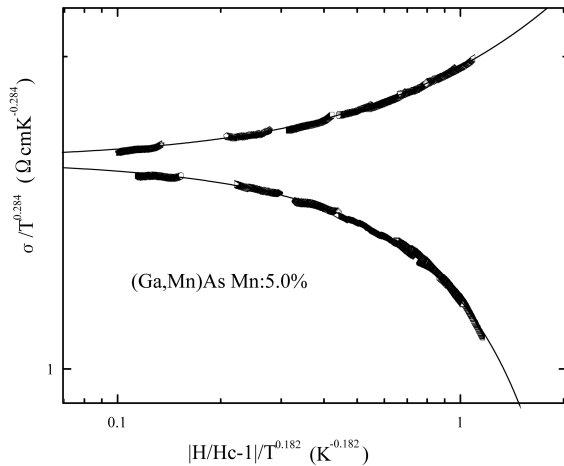


Fig.7 Results of fitting with two-parameter scaling scheme shown in the text for the second MIT in (Ga,Mn)As with $x=0.05$. The parameter is external magnetic field.

formula for the second MIT in (Ga,Mn)As with $x=0.05$ adopting a third-order polynomial for f . We found that this fitting is available for much wider region of parameters in the second MIT. This again supports the scenario presented in the previous subsection.

3. Summary

We have investigated the nature of ferromagnetism in (Ga,Mn)As and (In,Mn)As by utilizing LT-annealing effect. We propose a possible scenario for the ferromagnetism and two MITs in these materials.

Acknowledgments

This work was partly supported by a Grant-in-Aid for COE research (#12CE2004 ‘‘Control of Electrons by Quantum Dot Structures and Its Application to Advanced Electronics’’) and by a Grant-in-Aid for General Scientific Research from the Ministry of Education, Science, Sports and Culture of Japan.

- 1) H. Munekata, H. Ohno, S. von Molnar, A. Segmuller, L.L. Chang and L. Esaki: Phys. Rev. Lett. **63** (1989) 1849.
- 2) H. Ohno, A. Shen, F. Matsukura, A. Oiwa, A. Endo, S. Katsumoto and Y. Iye: Appl. Phys. Lett. **69**,(1996) 363.
- 3) S. Koshihara, A. Oiwa, M. Hirasawa, S. Katsumoto, Y. Iye, C. Urano, H. Takagi and H. Munekata: Phys. Rev. Lett. **78** (1997) 4617.
- 4) H. Ohno, D. Chiba, F. Matsukura, T. Omiya, E. Abe, T. Dietl, Y. Ohno and K. Ohtani: Nature **408** (2001) 944.
- 5) J. Inoue, S. Nonoyama, and H. Itoh: Phys. Rev. Lett. **85** (2000) 4610.
- 6) H. Shimizu, T. Hayashi, T. Nishinaga and M. Tanaka: Appl. Phys. Lett. **74** (1999) 398.
- 7) A. Shen, H. Ohno, F. Matsukura, Y. Sugawara, N. Akiba, T. Kuroiwa, A. Oiwa, A. Endo, S. Katsumoto and Y. Iye: J. Cryst. Growth **175/176** (1997) 1069.
- 8) T. Hayashi, Y. Hashimoto, S. Katsumoto and Y. Iye: Appl. Phys. Lett. **78** (2001) 1691.
- 9) T. Hayashi, Y. Hashimoto, S. Katsumoto and Y. Iye: to be published in Proc. 20th Int. Conf. Phys. Semicond.
- 10) S. O'Hagan and M. Missous: J. Appl. Phys. **75** (1994) 7835.
- 11) K. Hirakawa, S. Katsumoto, T. Hayashi, Y. Hashimoto and Y. Iye, submitted to Phys. Rev. **B**.
- 12) A. Oiwa, S. Katsumoto, A. Endo, M. Hirasawa, Y. Iye, H. Ohno, F. Matsukura, A. Shen and Y. Sugawara: Solid State Commun. **103** (1997) 209.